Charge measurement and mitigation for the main test-masses of the GEO 600 Gravitational Wave Observatory

M Hewitson[1], H Lück[1], H Grote[1], S Hild[1], S Rowan[2], J R Smith[1], K A Strain[1,2], B Willke[1]

[1] Max-Planck-Institut für Gravitationsphysik (Albert-Einstein-Institut) und Universität Hannover, Außenstelle Hannover, Callinstr. 38, 30167 Hannover, Germany.

[2] Department of Physics and Astronomy, University of Glasgow, Glasgow, G12 8QQ, United Kingdom

E-mail: martin.hewitson@aei.mpg.de

Abstract.

Charging of the test-masses in gravitational wave interferometers is a well known problem. Typically, concern arises due to the possibility of increased thermal noise due to a lowering of the quality factor of modes of the test-mass suspension, or due to the potential for increased displacement noise arising from charge migration on the surface of the test masses. Recent experience gained at the GEO 600 gravitational wave detector has highlighted an additional problem. GEO 600 uses electrostatic actuators to control the longitudinal position of the main test-masses. The presence of charge on the test-masses is shown to strongly affect the performance of the electrostatic actuators.

This paper reports on a measurement scheme whereby the charge-state of the GEO 600 test-masses can be measured using the electrostatic actuators. The resulting measurements are expressed in terms of an effective bias voltage on the electrostatic actuators. We also describe attempts to remove the charge from the test-masses and we show that the use of UV illumination was the most successful. Using UV illumination we were able to discharge and re-charge the test-masses.

1. Introduction

There are currently 6 kilometre-scale laser-interferometric Gravitational Wave (GW) detectors operational in the world: 3 detectors as part of the LIGO project [1]; a Japanese detector, TAMA 300 [2]; a French-Italian detector, VIRGO [3]; and a British-German collaboration, GEO 600 [4]. Together they form an international network searching for GWs from a variety of sources. All of these instruments are variations on a standard Michelson Interferometer, and all use large (of the order a few kilograms) suspended optics with high-reflectivity coatings as the mirrors that comprise the optical cavities. The optics whose differential length motion is what we detect at the dark-port of the Michelson (the mirrors at the ends of the arms for a standard Michelson), are typically called the test-masses. In all cases, the Michelson interferometers are operated at a dark-fringe and held there using actuators and active feedback control.

GEO 600 has many novel features compared to the other detectors. In the context of this paper, the most notable is the use of Electrostatic Drives (ESDs) as the main actuators for the test-masses. The ESDs

used in GEO 600 are implemented by having a gold electrode pattern deposited on the front surface of a reaction mass which is suspended behind the main test-mass. A schematic of the pendulum chain is given in Figure 1; a schematic of the electrode pattern coating mask is shown in Figure 2.

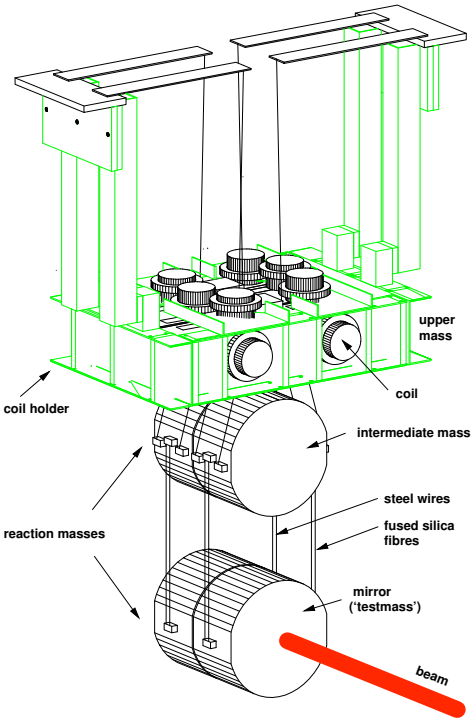

Figure 1. A schematic representation of the triple-pendulum chain from which are suspended the main test-masses of GEO 600.

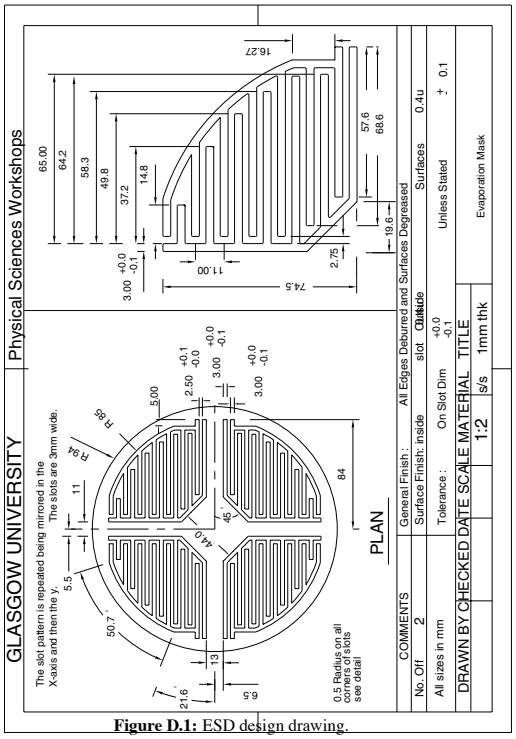

Figure D.1: ESD design drawing.

Figure 2. The design schematic for the GEO 600 ESD electrode coating mask.

By raising half of the electrodes to a high potential an electric field is generated which can pull on the dielectric test-mass. The force, F, exerted on the test-mass can be related to the voltage applied to the electrodes by

$$F = AV^2, \tag{1}$$

where A is a constant of proportionality related to the dielectric constant and relative dielectric constant of the test-mass, the spacing between the test-mass and the reaction mass (about 3 mm), and the geometry of the electrode pattern. For the GEO 600 ESDs, the gaps between the electrodes is about 2.5 mm, and the width of the electrodes is about 3 mm.

In order to achieve bipolar actuation, a bias voltage, V_{bias}, is applied to the electrodes so that the force becomes

$$F = A(V_{\mathrm{bias}} + V_s)^2, \tag{2}$$

where V_s is the actuation signal.

The displacement we achieve then depends on the bias voltage and the size of actuation signal. For frequencies well above the pendulum resonance ($f \gg 0.6\,\mathrm{Hz}$) and well below the first internal mode of the test-mass ($f \ll 10\,\mathrm{kHz}$), we can consider the test-mass as a rigid free mass. Then the displacement, x_ω, at angular frequency ω is related to the applied force by

$$F_\omega = -x_\omega m\omega^2, \tag{3}$$

where m is the mass of the test-mass. Therefore, we can relate the displacement at angular frequency ω to the applied bias and actuation voltage by

$$x(\omega) = \frac{A'}{\omega^2}(V_{\mathrm{bias}} + v(\omega))^2. \tag{4}$$

$$\tag{5}$$

If we apply an excitation signal $v(\omega_0) = V_0 \cos\omega_0$, then

$$x(\omega) = \frac{A'}{\omega_0^2}(V_{\mathrm{bias}} + V_0\cos\omega_0)^2, \tag{6}$$

$$= \frac{A'}{\omega_0^2}\left(V_{\mathrm{bias}}^2 + 2V_{\mathrm{bias}}V_0\cos\omega_0 + \frac{V_0^2}{2}(1+\cos 2\omega_0)\right), \tag{7}$$

$$\tag{8}$$

where V_0 is the amplitude of the signal at angular frequency ω_0 and the constant of proportionality, A', now incorporates the mass of the test-mass. If we discard the dc terms and those at $2\omega_0$ (since they don't contribute to the displacement at ω_0), we can write the resulting displacement as

$$x_{\omega_0} = 2\frac{A'}{\omega^2}V_{\mathrm{bias}}V_{\omega_0}, \tag{9}$$

where $V_{\omega_0} = v(\omega_0) = V_0\cos\omega_0$. In the remainder of this paper we will assume that all measurements are made at a single frequency, and drop the subscript 0 notation, just writing V_ω and x_ω instead.

2. Electrical charges on the test-masses

In GEO 600, the test-masses are suspended by fused-silica fibres from an intermediate fused-silica mass (which is itself suspended by steel wires from an upper mass). This is done so as to minimise the mechanical loss of the test-mass and hence keep the energy arising from Brownian motion constrained to narrow bands of frequencies. The result is that the test-masses are very well electrically isolated.

There are many mechanisms by which the test-masses of GEO 600 can become charged: through venting and evacuation of the vacuum chambers (friction); by allowing the test-mass to make electrical contact with the reaction-mass when the electrodes are held at their nominal bias voltage; accumulating charge from cosmic-ray interactions.

Having charged-up test-masses is not only bad from the point of view of noise [5, 6, 7, 8], but it also has a strong effect on the strength of electrostatic actuators which, in the case of GEO 600, means a change in the gain of the Michelson longitudinal servo, and, perhaps more importantly, a change to the absolute calibration of the main GW output which assumes constancy of the ESD strength over periods of several months (after initial calibration to another reference [9]).

Since the signal that we apply to the ESDs is non-symmetric (one electrode biased to $+600\,\mathrm{V}$; the other held at $0\,\mathrm{V}$), an additional electric field is created between the reaction mass and any surrounding

metal-work (for example, the vacuum tank walls); the strength of this field is proportional to the drive voltage we apply. If the test-masses then become charged to some potential, they experience a force due to this additional electric field. In contrast to the dielectric action described above, the force we exert here is proportional to the actuation signal since we can both push and pull the test-mass due to the charges on it. The resulting displacement produced by the electrostatic drive when the test-mass is charged can then be written as

$$x_\omega = 2\frac{A'}{\omega^2}V_{\text{bias}}V_\omega + \frac{\beta}{\omega^2}V_\omega \tag{10}$$

$$= \frac{2A'}{\omega^2}(V_{\text{bias}} + \beta')V_\omega, \tag{11}$$

where the constants of proportionality β and $\beta' = \beta/(2A')$ depend on the sign and amount of charge that is present on the test-mass as well as its distribution, the exact form of the electric field produced by this electrode/metal-work geometry, and, to a lesser extent, on the separation of the two masses. This is depicted in Figure 3.

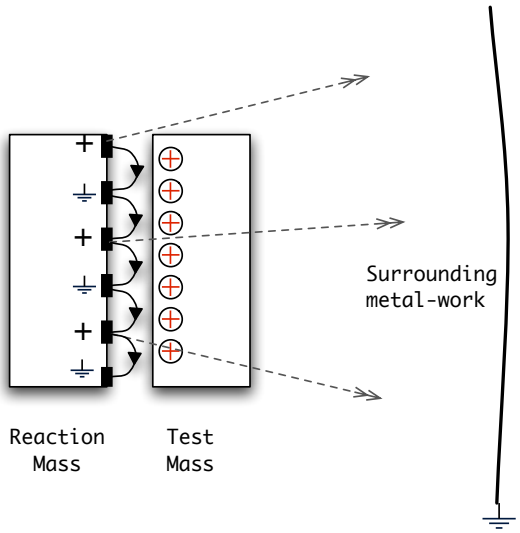

Figure 3. Schematic description of the field-lines that interact with charges on the test-mass. Here the fields lines emanate from the HV electrodes of the ESD and end on any extraneous metal-work.

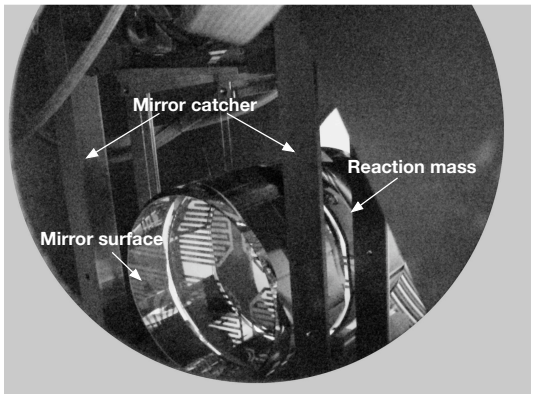

Figure 4. Photograph of the view of the East test-mass as seen from the UV lamp. The mirror (test-mass), reaction-mass and surrounding catcher are indicated.

From the second half of Equation 11 we can immediately see that, depending on the sign of β', the displacement we achieve for a given actuation signal will be either reduced or enhanced. We can think of β' as giving rise to an effective bias voltage, V_{eff}, and, as such, it is clear that there exists a value of the bias voltage, $V_{\text{bias}} = V_{\text{bias}_0}$, where the displacement we induce at frequency ω is zero‡. This immediately suggests a method to measure the charge present on the test-mass: for a given actuation signal, we can measure the displacement of the test-mass as a function of the bias voltage.

Once we have determined that a test-mass is charged, we want to remove (reduce) the charge. There are different courses of action that may achieve this, for example,

‡ The bias Voltage which produces no displacement is 0 V if the test-mass is fully discharged.

Venting This is a practical method for discharging optical components. In particular, for a negatively charged component we believe that venting is most effective if a gas of significant electron affinity, such as oxygen (in air), is used. For a positively charged component we believe that the most effective approach may again be to use a gas mixture, such as air, where there are often already negatively charged ions present. Alternatively, a gas of negative electron affinity, such as Argon, may be tried. We believe that if Argon is used (and is effective) there is the added advantage that the components should have less tendency to charge up as the gas is pumped out of the system.

UV illumination UV light of suitable wavelength can be used to remove electrons from the surface of a dielectric component thus removing excess negative charge. Alternatively the light can be shone on to a metal target near the mass and any positive charge on the mass can be neutralised by photoelectrons released from the metal. This method is employed in many experiments. See, for example, [10, 11, 12, 13].

Electrical contact Electrical charge can be removed from a local area of a mass by contact with an earthed conductor. However this method is not very effective for large and delicately suspended or mounted optical components.

2.1. Measuring the charge on the test-masses

As described in Section 2, the charge present on the test-mass can be evaluated by measuring the effective displacement a given actuation signal produces as a function of the dc bias voltage applied. Simplifying Equation 11 we get that the normalised (by the actuation signal) amplitude of the displacement we measure can be modelled by

$$\bar{x} = \frac{x_\omega}{V_\omega} = |aV_{\text{bias}} + b|, \tag{12}$$

where the constant a can be simply related to Equation 11 by $a = 2\frac{A'}{\omega^2}$, and the constant $b = 2\frac{A'\beta'}{\omega^2}$. Note that the two coefficients, a and b depend inversely on the square of the frequency of the drive signal. This relationship can be fit (in the least-squares sense) to the measured data to yield values for the two unknown coefficients. The effective bias, V_{eff}, due to charges on the test-mass is then given by the bias voltage needed to produce zero displacement. This is just

$$V_{\text{eff}} = -b/a. \tag{13}$$

Note that V_{eff} is just proportional to the charge on the test-mass and to the mass of the test-mass.

3. Case study: charging and discharging of the test-masses of GEO 600

During early December of 2006, a power cut at GEO 600 left the pendulums supporting the main test-masses un-damped. It is believed that, at the same time, the bias voltage was still supplied to the ESDs. While the nominal gap between test-mass and reaction mass is around 3 mm, the gap between the test-mass and the solder connections of the leads supplying the bias voltage to the ESD electrodes is much less, around 1 mm. This makes it highly likely that the test-mass can touch the reaction mass at these solder joints when the pendulum chain is un-damped.

After the power-cut, locking was not possible with normal parameters. After some investigation it became clear that the strength of the ESDs was significantly reduced (70% reduction for the East ESD,

and 30% for the North). We then investigated this further by connecting individual quadrants of the East ESD and measured the relative strengths to be 46%, 25%, 18%, and 12%. These measurements led to the thought that the test-masses were charged-up during the power-cut by touching the solder joints.

Measuring the charge on the East test-mass as described in Section 2.1 gives the trace shown in Figure 5. These measurements were made by injecting a signal at 696 Hz. The fit yields values for the coefficients of $a = -8 \times 10^{-6}$ and $b = 26.7 \times 10^{-4}$. From these values we get an effective bias due to charges of around 333 V.

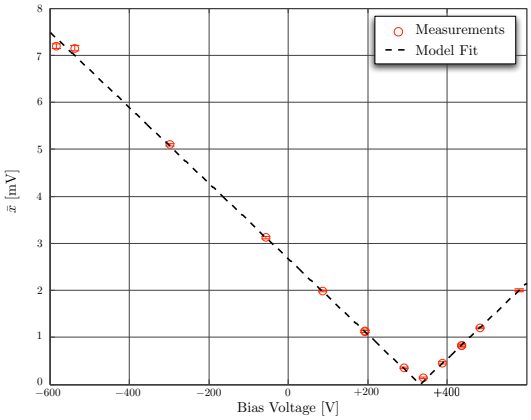

Figure 5. Measurement of the East test-mass charge-state after the power-cut. This measurement was made on 12 December 2006.

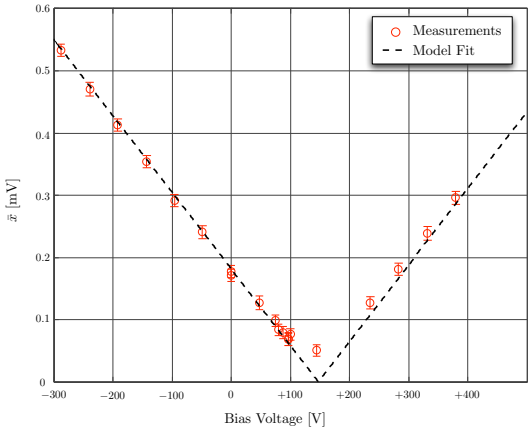

Figure 6. Measurement of the East test-mass charge-state after vacuum work. This measurement was made on 7 March 2007

Two attempts were made to remove the charges from the test-mass. The first attempt was to illuminate the test-mass with UV light from a source § placed external to the vacuum system and directed at the test masses through viewports on the vacuum system. The view of the test-mass as seen from the UV lamp is shown in Figure 4. The problem here is, at the time the relevant viewports were made from Kodial which transmits less than 2% of the incident UV. It turned out that we could not influence the charge-state of the test-mass after 1 hour of illumination. From this we deduced that discharging the test-mass in this way would take an unacceptably long time.

The second attempt was to flood the central vacuum cluster (which encloses the two test-masses), with Argon. The vacuum system was filled with about 1 mbar of Argon with the ESDs switched off. After evacuating the central cluster again, we remeasured the charge-state of the East test-mass and saw no significant change in the charge-state. We deduce that Argon at the low pressure used is not effective at discharging a positively charged component. In contrast to the major components of air (nitrogen and oxygen), which have a high electron affinity and would therefore be more suitable to remove negative charges, Argon, among the high purity gases we had available, has got a low ionisation threshold of 15.8eV compared to Helium (24.6eV) and Neon (21.5eV). The hope was that at pressures around 1 mbar and, correspondingly, low breakdown voltages, the electrical field of the charges present would sustain a short-duration glow-discharge, removing the charges from the mirror surface.

The commissioning plan of GEO 600 following the power-cut included opening the central cluster to re-position some beam-blocks. We decided that we would re-measure the charge-state of the two

§ Heraeus Noblelight: NK6-12, Mercury lamp with 800 mW output at 253.7 nm.

test-masses after this vacuum work, in the hope that venting to atmospheric pressure had removed the charges. In addition, the plan was to install Fused-Silica viewports which transmit close to 100% of any incident UV light. The vacuum system was opened on 21 February 2007, and following the central cluster work, the charge-state of the East test-mass was re-measured on 7 March 2007, this time using a signal frequency of 1234 Hz (this is about 85 days after the measurement shown in Figure 5). The results of this measurement are shown in Figure 6. The fit yields values for the coefficients of $a = -1.2 \times 10^{-6}$ and $b = 1.82 \times 10^{-4}$. From these values we get an effective bias due to charges of around 148 V. So, either the test-mass was not fully discharged while being in air (room temperature around 20°C, relative humidity of about 20%), or (more probably) the test-mass was charged again during the evacuation process.

With the new Fused-Silica viewports in place, the next step was to use UV illumination again to try and discharge the test-mass.

3.1. Discharging using UV light

The UV source described in Section 3 was used to illuminate the East test-mass. To monitor the discharging process, we injected a line into the East ESD at 1234 Hz and measured it at the output of the interferometer. Figure 7 shows the time-evolution of the amplitude of the injected line measured in a spectrum of the main interferometer output signal over the first 2 hours of the discharge process; during the period of illumination, the applied East test-mass bias was zero.

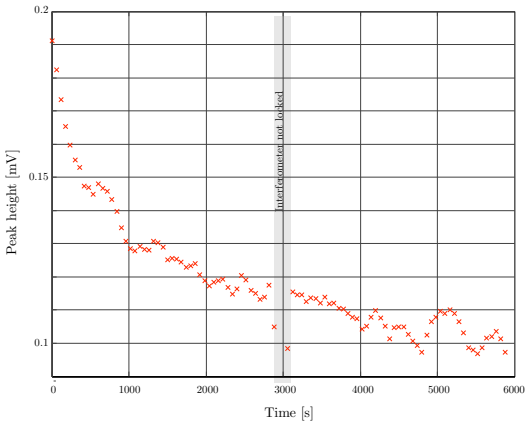

Figure 7. Tracking the strength of the East ESD during the discharge process via an injected line. The peak height is normalised by the power in the Power-Recycling cavity (*i.e.*, the optical gain).

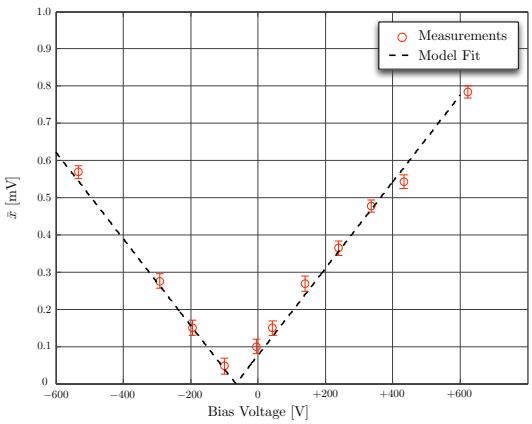

Figure 8. The charge-state measurement for the East test-mass after one night (around 15 hours) of UV illumination. The effective bias has gone from +148 V to −66 V in this time.

For the remaining period of illumination (13 hours), the detector was unlocked and the bias voltage was removed from the North ESD as well, since we don't know how the electric field from the bias voltage influences the discharging process.

Figure 8 shows the measurement of the charge-state of the East test-mass after overnight UV illumination (total of about 15 hours). The fit yields values of $a = -1.2 \times 10^{-6}$ and $b = -7.7 \times 10^{-5}$, which gives an effective bias voltage of -66 V. From this we can see that we have induced a negative effective bias during the illumination process. We deduce that we have released photoelectrons from the electrodes of the electrostatic drive and these have travelled to the near surface of the test mass.

The next experiment was to investigate the effect of UV illumination with the bias voltage switched on, with the hope that we could re-charge the test-mass to get an effective bias voltage close to zero Volts.

Suspecting that this process would be very sensitive to the illumination time and the bias voltage, we set the bias voltage to $+200\,\mathrm{V}$ and decided on 20 second illumination periods. To monitor progress, we injected a sinusoidal signal at 1234 Hz into the East ESD and measured its strength in the main detector output. From Figure 8 it is possible to compute the target line strength. At the beginning of the process, the line strength was measured to be around $410\,\mu$Vrms; the target line strength was computed to be $270\,\mu$Vrms. Figure 9 shows the individual measurements of the line strength for each burst of UV.

Figure 10 shows the measurement of MCe charge after re-charging. The fit to the measurements yields values of $a = -1.5 \times 10^{-6}$ and $b = 2.7 \times 10^{-5}$, which gives an effective bias voltage of 17.6 V. In this case we deduce that we have liberated electrons from the surface of the test mass and these have migrated to the appropriate electrode of the electrostatic drive under the applied electric field.

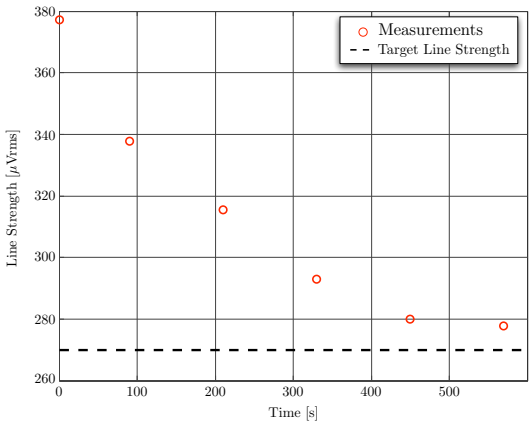

Figure 9. Measurements of the strength of injected 1234 H line during the recharging process.

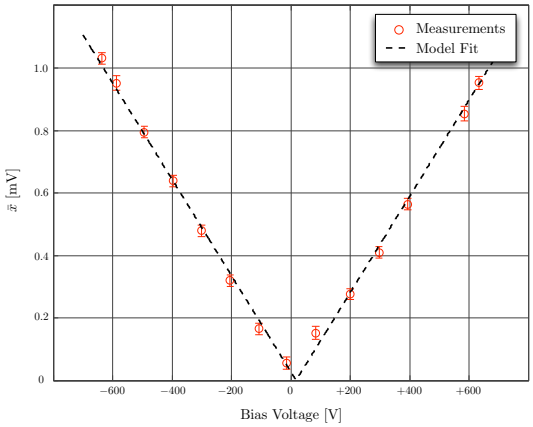

Figure 10. The charge-state measurement of the East test-mass after re-charging with UV and an applied bias voltage of $+200$ V.

4. Concluding remarks

Table 1 summarises the measurements presented in this paper. Note that the values for a in the fits should be independent of the charge and hence the same for all measurements made at the same frequency. In addition, the optical gain of GEO 600 is frequency dependent, so measurements made at different frequency not only scale by $1/\omega^2$, but also by the optical gain transfer function. This is the reason that the first measurement has a different value of a, since it was made at a different frequency. If we scale a from the first experiment by the square of the ratio of the frequencies $(696^2/1234^2)$ and by the ratio of the optical gain at these two frequencies $(0.6/1.5)$, we get a value of $a = -1.0 \times 10^{-6}$ which we can directly compare to the other measurements.

Our results presented here show clearly the efficacy of employing a UV light source for charge mitigation in an operating long-baseline gravitational wave interferometer. Since GEO 600 is an operational GW observatory, all detector investigations have to be carefully weighed for risk against damage and sensitivity reduction. As such, further charge experiments are not permitted on the instrument

Value of a	Value of b	$V_{\rm eff}$ [V]	Measurement details
$-8 \times 10{-}6$	$26.7 \times 10{-}4$	333	Measurement made after power-cut: 12 December 2006. Measurement frequency was 696Ḣz.
$-1.2 \times 10{-}6$	$1.82 \times 10{-}4$	148	Measurement made after vacuum work: 7 March 2007. Measurement frequency was 1234Ḣz.
$-1.2 \times 10{-}6$	$-7.7 \times 10{-}5$	-66	Measurement made after overnight UV illumination. Measurement frequency was 1234Ḣz.
$-1.5 \times 10{-}6$	$2.7 \times 10{-}5$	17.6	Measurement made after re-charging process with applied bias and UV illumination. Measurement frequency was 1234Ḣz.

Table 1. Summary of charge-state measurements made during the various experiments described throughout this paper.

once the charge state of the test-masses is returned to effectively zero. However there remain a number of open questions related to the use of UV for charge mitigation in interferometric detectors which require additional investigation and can be pursued in the laboratory. High, pulsed, laser-fluences of UV are known to cause damage in fused silica, hence studies of the effect of UV under similar conditions (wavelength, power, duration of illumination) used here on the optical properties of the substrates and coatings are of particular interest and under investigation in the laboratory [14]. In addition, for planned future generations of GW detectors, the implementation of methods of preventing the initial build-up of charge on the optics would be desirable. Thus, the appropriateness of various techniques is currently being assessed, including the use of thin coatings of conductive tin oxide [15] applied to the test masses and/or suspensions. The mechanical dissipation and optical absorption of such coatings to determine their suitability for this purpose is a subject of ongoing study.

Acknowledgments

The authors are grateful for support from PPARC and the University of Glasgow in the UK, and the BMBF and the state of Lower Saxony in Germany. This document has been assigned LIGO Laboratory document number LIGO-P070087-00-Z.

[1] *Status of LIGO at the start of the fifth science run*, Samuel J Waldman (for the LIGO Science Collaboration), Class. Quantum Grav. **23** No 19 (7 October 2006) S653-S660.
[2] *Current status of the TAMA300 gravitational-wave detector*, Masaki Ando and the TAMA Collaboration, Class. Quantum Grav. **22** No 18 (21 September 2005) S881-S889.
[3] *The Virgo status*, F Acernese *et al* , Class. Quantum Grav. **23** No 19 (7 October 2006) S635-S642.
[4] *The status of* GEO 600, S Hild (for the LIGO Scientific Collaboration), Class. Quantum Grav. **23** No 19 (7 October 2006) S643-S651.
[5] *Investigations into the effects of electrostatic charge on the Q factor of a prototype fused silica suspension for use in gravitational wave detectors*, S Rowan, S Twyford, R Hutchins and J Hough, 1997 Class. Quantum Grav. **14** 1537-1541.
[6] *Investigation of effects associated with variation of electric charge on a fused silica test mass*, V Mitrofanov, L Prokhorov, K Tokmakov and P Willems, Class. Quantum Grav. **21** No 5 (7 March 2004) S1083-S1089.
[7] *Description of charging/discharging processes of the LISA sensors*, Tim Sumner, Henrique Araújo, David Davidge, Alex Howard, Chris Lee, Geoff Rochester, Diana Shaul and Peter Wass, Class. Quantum Grav. **21** No 5 (7 March 2004) S597-S602.

[8] *Electrostatic charging of space-borne test bodies used in precision experiments*, Y Jafry, T J Sumner and S Buchman, 1996 Class. Quantum Grav. **13** A97-A106.
[9] *Principles of calibrating the dual-recycled GEO 600*, M Hewitson, G Heinzel, J R Smith, K A Strain, and H Ward, Rev. Sci. Instrum. 75, 4702 (2004).
[10] *LED deep UV source for charge management of gravitational reference sensors*, Ke-Xun Sun, Brett Allard, Saps Buchman, Scott Williams and Robert L Byer, Class. Quantum Grav. **23** (28 March 2006) S141-S150.
[11] *Charge measurement and control for the Gravity Probe B gyroscopes*, Saps Buchman, Theodore Quinn, G. M. Keiser, Dale Gill, and T. J. Sumner, Rev. Sci. Instrum. **66**, 120 (1995).
[12] *Testing of the UV discharge system for LISA Pathfinder*, P. J. Wass *et al* , AIP Conf. Proc. 873, 220 (2006).
[13] *The Charge-Management System on LISA-Pathfinder – Status & Outlook for LISA*, M. Schulte, G. K. Rochester, D. N. A. Shaul, T. J. Sumner, C. Trenkel, and P. J. Wass, AIP Conf. Proc. 873, 165 (2006).
[14] *Update of LIGO Test Mass Charging Mitigation Activities at Stanford*, K-X. Sun et al, LIGO document no: G070208-00-Z available at: http://admdbsrv.ligo.caltech.edu/dcc/.
[15] *The surface and materials science of tin oxide*, M. Batzill, U. Diebold, Progress in Surface Science **79** (2005) 47-154.